

# Quantification of regional $\dot{V}/\dot{Q}$ ratios in humans by use of PET. I. Theory

C. G. RHODES, S. O. VALIND, L. H. BRUDIN, P. E. WOLLMER, T. JONES, AND J. M. B. HUGHES

Medical Research Council Cyclotron Unit and Department of Medicine, Royal Postgraduate Medical School, Hammersmith Hospital, London W12 OHS, United Kingdom

RHODES, C. G., S. O. VALIND, L. H. BRUDIN, P. E. WOLLMER, T. JONES, AND J. M. B. HUGHES. *Quantification of regional  $\dot{V}/\dot{Q}$  ratios in humans by use of PET. I. Theory.* J. Appl. Physiol. 66(4): 1896–1904, 1989.—With positron emission tomography, quantitative measurements of regional alveolar and mixed venous concentrations of positron-emitting radioisotopes can be made within a transaxial section through the thorax. This allows the calculation of regional ventilation-to-perfusion ( $\dot{V}/\dot{Q}$ ) ratios by use of established tracer dilution theory and the constant intravenous infusion of  $^{13}\text{N}$ . This paper considers the effect of the inspiration of dead-space gas on regional  $\dot{V}/\dot{Q}$  and investigates the relationship between the measured  $\dot{V}/\dot{Q}$ , physiological  $\dot{V}/\dot{Q}$ , and  $\dot{V}/\dot{Q}$  defined conventionally in terms of bulk gas flow ( $\dot{V}_A/\dot{Q}$ ). Ventilation has been described in terms of net gas transport, and the term effective ventilation has been introduced. A simple two-compartment model has been constructed to allow for the reexpiration of regional (or personal) and common dead-space gas. By use of this model, with parameters representative of normal lung (see text), the effective  $\dot{V}/\dot{Q}$  ratio for  $^{13}\text{N}$  [ $(\dot{V}_A/\dot{Q})_{\text{eff}}(^{13}\text{N})$ ] is shown to overestimate  $\dot{V}_A/\dot{Q}$  by 18% when  $\dot{V}_A/\dot{Q} = 0.1$  but underestimate  $\dot{V}_A/\dot{Q}$  by 68% when  $\dot{V}_A/\dot{Q} = 10$ . For physiological gases, the model predicts that the behavior of  $\text{O}_2$  should be similar to that of  $^{13}\text{N}$ , so that, in terms of gas transport,  $\dot{V}/\dot{Q}$  ratios obtained using the infusion of  $^{13}\text{N}$  closely follow those for  $\text{O}_2$ . Values of the effective  $\dot{V}/\dot{Q}$  ratio for  $\text{CO}_2$  [ $(\dot{V}_A/\dot{Q})_{\text{eff}}(\text{CO}_2)$ ] lie approximately halfway between  $(\dot{V}_A/\dot{Q})_{\text{eff}}(^{13}\text{N})$  and  $\dot{V}_A/\dot{Q}$ . These results indicate that dead-space ventilation is far less a confounding issue when  $\dot{V}/\dot{Q}$  is considered in terms of net gas transport ( $\dot{V}_{\text{Aeff}}$ ), rather than bulk flow ( $\dot{V}_A$ ). Finally, the existence of  $\dot{V}/\dot{Q}$  heterogeneity within the resolution element of the scanner results in a divergence between the measured  $\dot{V}/\dot{Q}$  and the volume- or blood flow-weighted  $\dot{V}/\dot{Q}$  ratios, the magnitude varying between 0 and 40% for a twofold variation in heterogeneity, depending on the volume distribution of  $\dot{V}/\dot{Q}$  within the volume element.

gas transport; regional lung function; inert gas elimination

THE IMPORTANCE of adequate matching between ventilation ( $\dot{V}$ ) and perfusion ( $\dot{Q}$ ), for the lung to function effectively as a gas-exchanging organ, has motivated many workers to investigate the diversity of ventilation-to-perfusion ( $\dot{V}/\dot{Q}$ ) relationships in humans. Regional  $\dot{V}/\dot{Q}$  measurements have been made noninvasively using radiolabeled tracers and external radiation detection. Anthonisen et al. (1) used the continuous intravenous infusion of  $^{133}\text{Xe}$  and existing steady-state theory to derive regional values of  $\dot{V}/\dot{Q}$  by recording the regional

distribution of activity with an external detector array. This approach was limited by a number of technical and theoretical uncertainties, not least the inability to measure true regional isotope concentration, which resulted in a degree of ambiguity in the interpretation of the measured  $\dot{V}/\dot{Q}$  distribution. Independent measurements of  $\dot{V}$  and  $\dot{Q}$  have also been used to map out regional  $\dot{V}/\dot{Q}$  ratios (5, 8), but problems of quantification arise in the determination of isotope concentration.

In this paper, we consider the implications for regional  $\dot{V}/\dot{Q}$  measurements stemming from the technological development of positron emission tomography (9). This instrumentation allows mixed venous and regional alveolar concentrations of an infused inert gas radionuclide ( $^{13}\text{N}$ ) to be measured precisely in three dimensions, under well-defined geometric conditions, as described in the companion paper (10). The questions we address here in a quantitative manner concern 1) the reexpiration of alveolar gas into the local volume element from other lung regions (i.e., by virtue of the inspiration of alveolar gas from the anatomical dead space, denoted here as dead-space ventilation) and its effect on the net transport of gas, 2) the way in which such effects of dead-space ventilation vary with the solubility of the gas being studied, 3) the relationship between the  $\dot{V}/\dot{Q}$  measured with  $^{13}\text{N}$  and that pertaining to the more soluble physiological gases,  $\text{O}_2$  and  $\text{CO}_2$ , 4) the effect of microscopic  $\dot{V}/\dot{Q}$  heterogeneity within the volume element on the measured volume-weighted regional  $\dot{V}/\dot{Q}$  distribution, and 5) the propagation of error in the measurement of  $\dot{V}/\dot{Q}$ .

## Glossary

$\dot{V}_T$	Total expiratory ventilation of the volume element
$\dot{V}_D$	Total dead-space ventilation of the volume element
$\dot{V}_{D_i}$	Dead-space ventilation by gas originating from a region $i$ ( $\dot{V}_D = \sum \dot{V}_{D_i}$ )
$\dot{V}_A$	Alveolar ventilation ( $\dot{V}_A = \dot{V}_T - \dot{V}_D$ )
$\dot{Q}_j$	Blood flow (perfusion) of region $j$
$\dot{V}/\dot{Q}$	Ventilation-to-perfusion ratio (general)
$(\dot{V}_A/\dot{Q})_j$	Conventional $\dot{V}/\dot{Q}$ ratio of region $j$ defined in terms of alveolar ventilation

$(\dot{V}_A/\dot{Q})_{\text{eff}(y)_j}$	$\dot{V}/\dot{Q}$ ratio of <i>region j</i> for gas <i>y</i> , defined in terms of effective alveolar ventilation (see <i>Eqs. A3</i> and <i>A5</i> )
$CD_i(y)$	Isotope concentration of gas <i>y</i> ( $\mu\text{Ci/ml}$ gas) in dead-space <i>region i</i>
$CA_j(y)$	Isotope concentration of gas <i>y</i> ( $\mu\text{Ci/ml}$ gas) in alveolar gas of <i>region j</i>
$P_j(y)$	Partial pressure of gas <i>y</i> in <i>region j</i>
<i>x</i>	Ideal gas ( <i>x</i> )
$\lambda_x$	Ostwald solubility coefficient of gas <i>x</i>
<i>A</i>	Alveolar
$D_r$	Regional dead space
$D_c$	Common dead space
<i>r</i>	Subscript referring to the region of interest
<i>e</i>	Subscript referring to the lung outside the volume element of the region of interest
atm	Atmospheric
$F_c$	Constant of proportionality between $\dot{V}D_c$ and $\dot{V}_A$ (i.e., $F_c = \dot{V}D_c/\dot{V}_A$ )

**THEORY**

The technique is based on the conservation of tracer at the alveolar capillary-gas interface, as expressed by the Fick principle (7), during the constant intravenous infusion of dissolved radioisotopic  $^{13}\text{N}$ . In deriving the model the following assumptions are made. 1) The volume element of lung analyzed within the tomographic section (pixel volume) is homogeneous with respect to matching between ventilation and blood flow (i.e.,  $\dot{V}/\dot{Q}$  is uniform). 2) During the intravenous infusion of  $^{13}\text{N}$ , there is a continuous supply of tracer to all lung regions at a mixed venous concentration ( $C_{\bar{v}}$ ) equal to that in the right ventricle ( $^{13}\text{N}$  is infused from a fixed activity reservoir at constant flow; thus all concentrations of  $^{13}\text{N}$  must be corrected for radioactive decay,  $T_{1/2} = 10$  min). 3) Blood flow and ventilation are not pulsatile and tidal but continuous processes that are invariant for the duration of the study. This implies that regional alveolar

volume ( $V_A$ ) does not vary throughout the respiratory cycle. 4) There is true equilibrium of the tracer between end-capillary blood and alveolar gas, and the distribution of tracer within the alveolus is uniform.

*Mathematical model.* During the continuous intravenous infusion of the inert gas isotope  $^{13}\text{N}$  [blood-to-gas partition coefficient,  $\lambda_N = 0.015$  (6)] activity arriving at the lung 1) partitions between the alveolar gas and capillary blood and 2) is removed from the region by both ventilation and blood flow (3). Because of the low blood solubility of  $\text{N}_2$  the bulk of the activity is removed by ventilation, and the recirculation of tracer is low.

At the start of each inspiration, however, activity remaining in the ventilatory dead space will reenter alveoli before the inspiration of fresh gas from the atmosphere. The  $^{13}\text{N}$  content of the dead-space gas will vary according to its location in the airways, since it will be determined by the concentration of gas expired from a number of lung regions with different  $\dot{V}/\dot{Q}$  ratios. The dead-space gas close to a terminal airway may have a  $^{13}\text{N}$  concentration similar to the alveolar gas of that region, whereas dead-space gas in larger airways will have a concentration equal to the ventilation-weighted mean concentration of the lung regions subtended. For a given volume element of lung ( $V_L$ ) the inspired dead-space activity can be considered to be made up from a number ( $n$ ) of different fractions, each originating from individual dead-space *regions i* (where  $i$  runs from 1 to  $n$ ). Therefore the total  $^{13}\text{N}$  activity inspired by the region is equal to the sum  $\sum \dot{V}D_i CD_i$  where  $\dot{V}D_i$  is the ventilation by gas from a dead-space *region i*, with a  $^{13}\text{N}$  concentration equal to the concentration of gas in the dead-space *region i* ( $CD_i$ ). This model is shown diagrammatically in Fig. 1.

By applying the Fick principle to a volume element of lung within the tomographic section, a steady-state equation can be formulated that equates the rate of arrival of tracer ( $\dot{Q}C_{\bar{v}} + \sum \dot{V}D_i CD_i$ ) to the rate of removal by ventilation ( $\dot{V}_T CA$ ) and blood flow ( $\dot{Q}C_c'$ ) at equilibrium.  $\dot{Q}$  is the blood flow to the region,  $\dot{V}_T$  is the total expiratory ventilation of the region, and  $CA$  and  $C_c'$  are the alveolar and end-capillary blood concentrations of  $^{13}\text{N}$ , respectively. Because  $C_c' = \lambda_N CA$  (see *assumption 4* and the

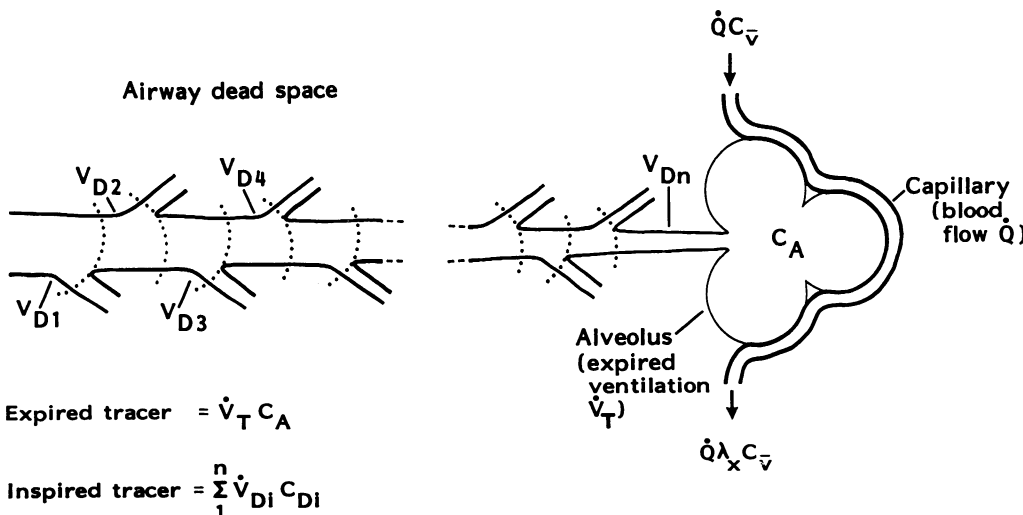


FIG. 1. Model of gas transport at alveolar level. Tracer is taken to and removed from alveolus both by blood flow ( $\dot{Q}$ ) and ventilation ( $\dot{V}$ ). Each dead-space region ( $i$ , where  $i$  runs from 1 to  $n$ ) is associated with a volume ( $V_{D_i}$ ) and a tracer concentration ( $CD_i$ , see text for mass-balance equation).  $\lambda_x$ , Ostwald solubility coefficient for an inert gas ( $x$ ).

definition of the Ostwald solubility coefficient), the following equation can be written

$$\dot{Q}C\bar{v} + \sum \dot{V}D_i CD_i = \dot{V}_T CA + \dot{Q} \lambda_N CA \quad (1)$$

For practical purposes, this equation can first be simplified by introducing the concept of effective dead-space ventilation, a parameter that is dependent on the difference between the  $^{13}\text{N}$  concentrations of alveolar and dead-space gas. For example, a lung region with a low  $\dot{V}/\dot{Q}$  ratio may be partly ventilated by dead-space gas originating from a lung region with a normal or high  $\dot{V}/\dot{Q}$  ratio, in which case the dead-space gas contains  $^{13}\text{N}$  at a lower concentration than that of the alveolus. The dead-space ventilation then represents useful ventilation to the extent that it facilitates removal of  $^{13}\text{N}$  from the alveolus and thus corresponds to a significant ventilation in addition to the alveolar ventilation ( $\dot{V}_A$ ). Conversely, a high  $\dot{V}/\dot{Q}$  region ventilated by dead-space gas from a region with a lower  $\dot{V}/\dot{Q}$  will not exchange  $^{13}\text{N}$  as well as expected, because the dead-space gas now contains more  $^{13}\text{N}$  (per unit gas volume) than the local alveolar gas. This results in an effective dead-space ventilation ( $\dot{V}D_{\text{eff}}$ ), which is larger than the physical dead-space ventilation, i.e.,  $\dot{V}D_{\text{eff}} > \sum \dot{V}D_i$ .

$\dot{V}D_{\text{eff}}(^{13}\text{N})$  is thus defined as that ventilation which would be necessary to transport the "local share" of the total dead-space activity ( $\sum \dot{V}D_i CD_i$ ) into the region of interest at a constant  $^{13}\text{N}$  concentration equal to that of the "resident" alveolar gas,  $CA$ . This can be expressed mathematically as

$$\dot{V}D_{\text{eff}}(^{13}\text{N}) CA = \sum \dot{V}D_i CD_i \quad (2)$$

This represents a scaling of the true dead-space ventilation ( $\dot{V}D$ ), according to the amount of  $^{13}\text{N}$  carried by the gas. In this respect,  $\dot{V}D$  is not assessed mechanically, solely in terms of gas flow, but functionally, in terms of gas transport. From Eq. 2 follows the definition of effective alveolar ventilation for  $^{13}\text{N}$

$$\dot{V}A_{\text{eff}}(^{13}\text{N}) = \dot{V}_T - \dot{V}D_{\text{eff}}(^{13}\text{N}) \quad (3)$$

(This contrasts with the conventional definition of  $\dot{V}A$  in that  $\dot{V}D_{\text{eff}}(^{13}\text{N})$  replaces  $\dot{V}D$ . But clearly, when  $CD_i = CA$ , then  $\dot{V}A_{\text{eff}}(^{13}\text{N}) = \dot{V}A$ .) Substituting Eqs. 2 and 3 into Eq. 1 to eliminate  $\sum \dot{V}D_i CD_i$  and  $\dot{V}_T$  and rearranging gives the operational equation

$$(\dot{V}A/\dot{Q})_{\text{eff}}(^{13}\text{N}) = C\bar{v}/CA - \lambda_N \quad (4)$$

(This equation, relating alveolar ( $CA$ ) and mixed venous ( $C\bar{v}$ ) (concentration of tracer) to  $\dot{V}/\dot{Q}$ , should not be confused with a similar equation also defined in terms of concentration but involving arterial retention of tracer, viz  $CA = \lambda C\bar{v}/(\lambda + \dot{V}/\dot{Q})$ , or the commonly used equation defined in terms of partial pressures (13) i.e.,  $P_a = \lambda P\bar{v}/(\lambda + \dot{V}/\dot{Q})$ . (Noting  $P_a/P\bar{v} = CA/C\bar{v}$ , see below). Because  $P_a = P_A$  (if assumption 4 holds),  $P_A = 760CA$  and  $P\bar{v} = 760C\bar{v}/\lambda$  (this relationship derives directly from the definition of  $\lambda$ ), then  $P_a/P\bar{v} = P_A/P\bar{v} = \lambda CA/C\bar{v}$ . This can be substituted into the retention equation to give an equation in the form of Eq. 4.)

The application of Eq. 4 to the regional measurement of  $\dot{V}/\dot{Q}$  ratio requires the steady-state measurement of

regional alveolar  $^{13}\text{N}$  concentration ( $CA_r$ ) and  $C\bar{v}$  during the continuous intravenous infusion of  $^{13}\text{N}$  in saline. The details of this procedure, a discussion of experimental uncertainties, and results of measurements made in normal subjects are presented in the companion paper (10).

#### ASSESSMENT OF MODEL

*Relationship between effective and alveolar  $\dot{V}/\dot{Q}$ .* For a given inert gas tracer ( $x$ ), differences between effective alveolar ventilation of  $x$  [ $\dot{V}A_{\text{eff}}(x)$ ] and  $\dot{V}A$  occur when gas, inhaled as part of  $\dot{V}D$ , has a tracer composition different from the alveolar gas of the region of interest. This results from the reexpiration of gas from regions with  $\dot{V}/\dot{Q}$  ratios different from that of the region of interest. However, the situation is further complicated, since the  $CA$  of an inert gas tracer is dependent not only on the  $\dot{V}/\dot{Q}$  of the region but also on the solubility of the tracer (see Eq. 4). Therefore effective ventilation is dependent on the gas in question, whether it be an inert gas tracer or one of the physiological gases. Hence, in any given situation, effective alveolar ventilation ( $\dot{V}A_{\text{eff}}$ ) will have different values for  $^{13}\text{N}$ ,  $\text{O}_2$ , and  $\text{CO}_2$ . A comparison between  $\dot{V}A_{\text{eff}}$  and  $\dot{V}A$ , in terms of the respective  $\dot{V}/\dot{Q}$  ratios, can be made by considering a simple lung model where  $\dot{V}D$  is either regional (i.e., personal), with a gas composition identical to the alveolar gas of the region of interest, or common, with a gas composition determined by the lung outside the region of interest. Such a model is described in APPENDIX 1. Relationships between  $(\dot{V}A/\dot{Q})_{\text{eff}}$  and the  $\dot{V}/\dot{Q}$  ratio defined in terms of alveolar ventilation ( $(\dot{V}A/\dot{Q})_r$ ) for the volume element in the region of interest ( $r$ ) were calculated for  $^{13}\text{N}$ ,  $\text{O}_2$ , and  $\text{CO}_2$  by use of Eqs. A5, A8, and A3, respectively. In this model the simplifying assumption was made that the respiratory exchange ratio ( $RQ$ ) was unity for each lung region (see derivation of model, APPENDIX 1). The composition of gas in the common dead space was chosen to be representative of normal lung and thus originate from a single lung region (external to the volume element) with a  $\dot{V}/\dot{Q}$  ratio [ $(\dot{V}A/\dot{Q})_e$ ] equal to 0.75. Total  $\dot{V}D$  was taken to be 30% of  $\dot{V}_T$ , and regional and common dead-space ventilations ( $\dot{V}D_r$  and  $\dot{V}D_c$ , respectively) were chosen to be equal. Thus the value of the common dead-space ventilatory fraction  $F_c$  ( $= \dot{V}D_c/\dot{V}A$ , see Glossary) was 0.214 ( $= 0.15/0.70$ ). Alveolar partial pressures of  $\text{O}_2$  and  $\text{CO}_2$  were calculated using the multiple-compartment  $\dot{V}/\dot{Q}$  computer program (VQMODEL) of West and Wagner (14). The effective inspired partial pressures ( $P_{\text{eff}}$ ) of  $\text{O}_2$  or  $\text{CO}_2$  were calculated, as a function of  $(\dot{V}A/\dot{Q})_r$ , using simple dilution principles (see APPENDIX, Eq. A6). The  $\dot{V}/\dot{Q}$  program was thus used iteratively to calculate alveolar  $PO_2$  and  $PCO_2$  for a  $(\dot{V}A/\dot{Q})_r$  ratio of 0.75 (to provide common dead-space partial pressures of the two gases) and for  $(\dot{V}A/\dot{Q})_r$  ratios ranging from 0.1 to 50 [to provide regional dead-space partial pressures and alveolar partial pressures for subsequent use in Eqs. A3 (modified for partial pressure) and A8]. For each run of the program, the mixed venous  $PO_2$  and  $PCO_2$  were fixed at  $40.0 \pm 0.1$  and  $45.0 \pm 0.1$  Torr, respectively. (This was achieved mainly by altering the  $\dot{V}_T$  to the lung model but also by allowing the  $RQ$  of the lung to vary between

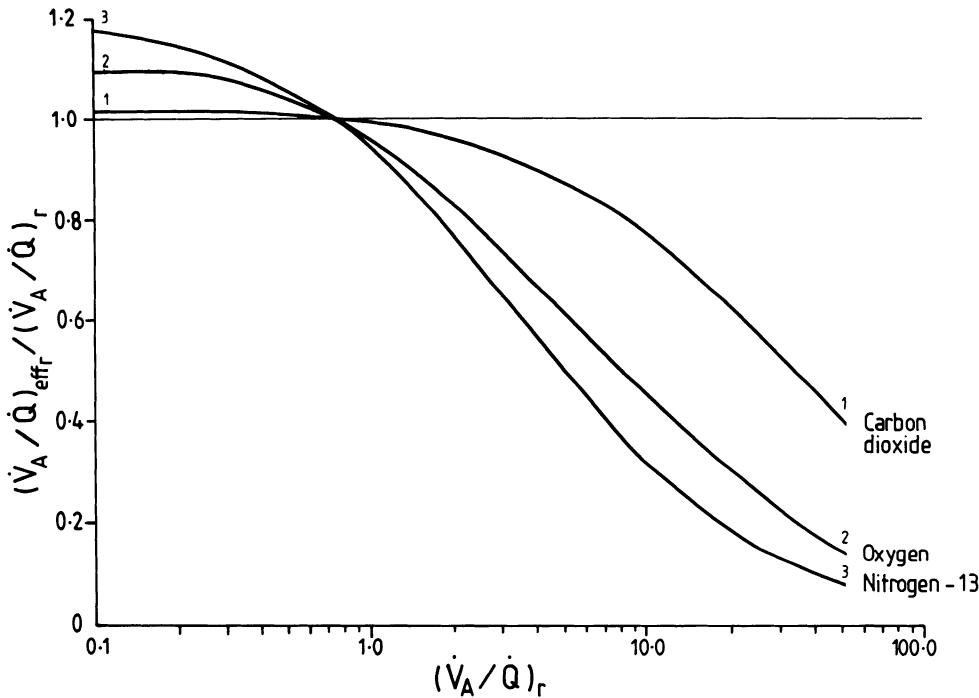


FIG. 2. Graphical relationship between  $(\dot{V}_A/\dot{Q})_{\text{eff},r}/(\dot{V}_A/\dot{Q})_r$  and  $(\dot{V}_A/\dot{Q})_r$  for an ideal inert gas ( $\lambda = 0.015$ ,  $N_2$ ),  $O_2$ , and  $CO_2$ . Total dead-space ventilation ( $\dot{V}_D$ ) was chosen to equal 0.3 of the total expiratory ventilation ( $\dot{V}_T$ ) and comprise regional ( $\dot{V}_{D,r}$ ) and common ( $\dot{V}_{D,c}$ ) dead-space fractions (where  $\dot{V}_{D,r} = \dot{V}_{D,c}$ ).  $\dot{V}/\dot{Q}$  ratio of external lung region supplying gas to the common dead space  $[(\dot{V}_A/\dot{Q})_e]$  was assigned a value of 0.75.

0.78 and 0.85). Atmospheric  $PO_2$  and  $PCO_2$  were fixed at 150 and 0 Torr, respectively. The mixed venous partial pressure of  $N_2$  was chosen such that no net transfer of this gas occurred. The following parameters were also fixed: atmospheric pressure = 760 Torr, body temperature =  $37^\circ C$ , hemoglobin = 0.148 g/ml, acid-base excess = 0, and hematocrit = 0.45.

The relationship between  $(\dot{V}_A/\dot{Q})_{\text{eff},r}$  and  $(\dot{V}_A/\dot{Q})_r$  is shown in Fig. 2 where the ratio  $(\dot{V}_A/\dot{Q})_{\text{eff},r}/(\dot{V}_A/\dot{Q})_r$  has been plotted against  $(\dot{V}_A/\dot{Q})_r$  for  $^{13}N$  ( $\lambda_x = 0.015$ ),  $O_2$ , and  $CO_2$ . A progressive divergence between  $(\dot{V}_A/\dot{Q})_{\text{eff},r}$  and  $(\dot{V}_A/\dot{Q})_r$  can be seen as the difference between  $(\dot{V}_A/\dot{Q})_r$  and  $(\dot{V}_A/\dot{Q})_e$  increases. The magnitude of this effect increases as the solubility of the gas decreases. Thus, when  $(\dot{V}_A/\dot{Q})_r = 0.1$ ,  $(\dot{V}_A/\dot{Q})_{\text{eff},r}$  exceeds  $(\dot{V}_A/\dot{Q})_r$  by 2, 10, and 18% for  $CO_2$ ,  $O_2$ , and  $^{13}N$ , respectively, and when  $(\dot{V}_A/\dot{Q})_r = 10$ ,  $(\dot{V}_A/\dot{Q})_{\text{eff},r}$  falls below  $(\dot{V}_A/\dot{Q})_r$  by 23, 55, and 68%, respectively, for the three gases. At this point there is almost a twofold difference between  $(\dot{V}_A/\dot{Q})_{\text{eff},r(O_2)}$  and  $(\dot{V}_A/\dot{Q})_{\text{eff},r(CO_2)}$ . As  $(\dot{V}_A/\dot{Q})_r$  falls to a value much less than  $(\dot{V}_A/\dot{Q})_e$ , the ratio  $(\dot{V}_A/\dot{Q})_{\text{eff},r}/(\dot{V}_A/\dot{Q})_r$  approaches a limiting value of  $[(1 + F_c)(\dot{V}_A/\dot{Q})_e + \lambda_x]/[(\dot{V}_A/\dot{Q})_e + \lambda_x]$  for an ideal gas (x). This limit is approximately equal to  $[\dot{V}_{A,r} + \dot{V}_{D,c}]/\dot{V}_{A,r}$  (i.e.,  $(1 + F_c)$ ) for a gas of very low solubility and has a numerical value of 1.21 for the parameters used in this example. As the value of  $(\dot{V}_A/\dot{Q})_r$  increases beyond  $(\dot{V}_A/\dot{Q})_e$ ,  $(\dot{V}_A/\dot{Q})_{\text{eff},r}$  progressively underestimates  $(\dot{V}_A/\dot{Q})_r$ , and the ratio tends asymptotically to zero.

An important characteristic of  $(\dot{V}_A/\dot{Q})_{\text{eff},r}$ , when regional blood flow ( $\dot{Q}_r$ ) is very low, can be observed by plotting  $(\dot{V}_A/\dot{Q})_{\text{eff},r}$  and  $(\dot{V}_A/\dot{Q})_r$  vs.  $\dot{Q}_r$  (using Eq. A5) while assigning an arbitrary constant value of 0.7 ml/min to  $\dot{V}_A$  and maintaining  $(\dot{V}_A/\dot{Q})_e = 0.75$ . This is shown in Fig. 3 where the familiar hyperbolic relationship between  $(\dot{V}_A/\dot{Q})_r$  and  $\dot{Q}_r$  is seen. In absolute terms,

$(\dot{V}_A/\dot{Q})_{\text{eff},r}$  is only slightly greater than  $(\dot{V}_A/\dot{Q})_r$  for low  $\dot{V}/\dot{Q}$  (high  $\dot{Q}_r$ ) regions [i.e., when  $(\dot{V}_A/\dot{Q})_r \ll (\dot{V}_A/\dot{Q})_e$ ], the ratio reaching the limiting value of 1.21 for the parameters used in this example (see above). However,  $(\dot{V}_A/\dot{Q})_{\text{eff},r}$  progressively underestimates  $(\dot{V}_A/\dot{Q})_r$  for low values of  $\dot{Q}_r$ , reaching a finite maximum value, as  $\dot{Q}_r$  tends toward zero, of  $[(1 + F_c)(\dot{V}_A/\dot{Q})_e + \lambda_x]/F_c$ , which, in this example, is equal to 4.32. The corresponding maximum value for  $(\dot{V}_A/\dot{Q})_{\text{eff},r(O_2)}$ , would be 8.0, with the assumption of an effective solubility coefficient for  $O_2$  of 0.8 (see DISCUSSION).

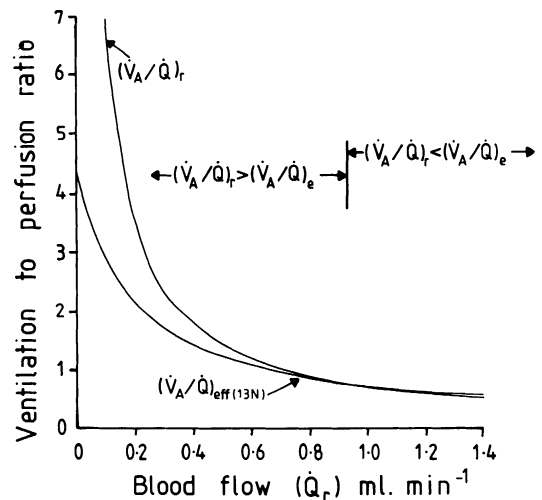


FIG. 3. Relationship between effective dead-space ventilation for  $^{13}N$  in region of interest  $[(\dot{V}_A/\dot{Q})_{\text{eff},r}]$ ,  $(\dot{V}_A/\dot{Q})_r$ , and blood flow ( $\dot{Q}_r$ ) for a region (r). Values of 0.75 and 1.0 ml/min were assigned to  $(\dot{V}_A/\dot{Q})_e$  and  $\dot{V}_T$ , respectively ( $\dot{V}_{A,r} = 0.7 \dot{V}_T$ ).  $(\dot{V}_A/\dot{Q})_r$  exhibits the expected hyperbolic relationship with  $\dot{Q}_r$ , whereas  $(\dot{V}_A/\dot{Q})_{\text{eff},r}$  increases more slowly as  $\dot{Q}_r$  falls, reaching a maximum value of 4.32 for the parameters chosen in this example. See Fig. 2 legend for definitions of other abbreviations.

*Heterogeneity of  $\dot{V}/\dot{Q}$  within the volume element.* Under conditions of microscopic  $\dot{V}/\dot{Q}$  mismatching, an averaging of the individual  $\dot{V}/\dot{Q}$  ratios within the volume element occurs. This results in a measured  $\dot{V}/\dot{Q}$  ratio that is virtually equal to the reciprocal of the volume-weighted mean  $\dot{Q}/\dot{V}$  for that region (see APPENDIX, Eq. A13). However, this mean  $\dot{V}/\dot{Q}$  ratio may differ considerably from the true volume-weighted mean  $\dot{V}/\dot{Q}$  ratio, or for that matter, the blood flow- or ventilation-weighted means as obtained by use of the multiple inert gas elimination technique of Wagner (13).

In this section, predicted values of the mean  $\dot{V}/\dot{Q}$  obtained by use of external detection and the  $^{13}\text{N}$  elimination approach [ $(\dot{V}/\dot{Q})_{\text{Ext}}$ ] are compared with volume- and blood flow-weighted means,  $(\dot{V}/\dot{Q})_{\dot{Q}}$  and  $(\dot{V}/\dot{Q})_{\dot{V}}$ , respectively, for a lung region containing various degrees of  $\dot{V}/\dot{Q}$  heterogeneity. (To simplify this analysis, dead-space effects have been omitted, and the  $\dot{V}/\dot{Q}$  ratios used are therefore unsubscripted and refer to  $\dot{V}_A$  where all  $\dot{V}D$  is assumed to be at regional concentrations). Volume- and blood flow-weighted means have been chosen because the former corresponds to the way in which we approach the interregional analysis of  $\dot{V}/\dot{Q}$ , and the latter relates  $\dot{V}T$  to total blood flow in a region and thereby allows the calculation of  $\dot{Q}_r$  from measured values of  $\dot{V}$  and  $\dot{V}/\dot{Q}$  by use of the simple relationship  $\dot{Q} = \dot{V}/(\dot{V}/\dot{Q})$ . The mathematical derivations are shown in APPENDIX 2.

Differences between  $(\dot{V}/\dot{Q})_{\text{Ext}}$ ,  $(\dot{V}/\dot{Q})_{\dot{V}}$ , and  $(\dot{V}/\dot{Q})_{\dot{Q}}$  have been investigated by considering the extreme but pathologically realistic case of a volume element of lung with two single populations of  $\dot{V}/\dot{Q}$ ,  $(\dot{V}/\dot{Q})_1$  and  $(\dot{V}/\dot{Q})_2$ . Associated with the two subregions are independent values of blood flow,  $\dot{Q}_1$ , and  $\dot{Q}_2$ ; ventilation,  $\dot{V}_1$  and  $\dot{V}_2$ ; and

thoracic volume,  $V_1$  and  $V_2$ .  $(\dot{V}/\dot{Q})_2$  has been assigned a value of unity, whereas the value of  $(\dot{V}/\dot{Q})_1$  has been varied between zero and six. Because this variation of  $(\dot{V}/\dot{Q})_1$  can arise either from changes in  $\dot{V}$  or  $\dot{Q}$ ,  $(\dot{V}/\dot{Q})_{\dot{Q}}$  has been defined both for equal  $\dot{V}$  to the subregions ( $\dot{V}_1 = \dot{V}_2$ ,  $\dot{Q}_1$  varies) and equal blood flow ( $\dot{Q}_1 = \dot{Q}_2$ ,  $\dot{V}_1$  varies). Three relationships between  $V_1$  and  $V_2$  have been chosen 1)  $V_1 = 10V_2$ , 2)  $V_1 = V_2$ , and 3)  $10V_1 = V_2$ .

To determine the relationships between the averaged  $\dot{V}/\dot{Q}$  ratio measured in the volume element and the mean  $\dot{V}/\dot{Q}$  ratios, weighted for blood flow or volume, the ratios  $(\dot{V}/\dot{Q})_{\text{Ext}}/(\dot{V}/\dot{Q})_{\dot{Q}}$  and  $(\dot{V}/\dot{Q})_{\text{Ext}}/(\dot{V}/\dot{Q})_{\dot{V}}$  were calculated as a function of the ratio  $(\dot{V}/\dot{Q})_1/(\dot{V}/\dot{Q})_2$  and are shown plotted in Fig. 4. From these diagrams, considerable differences between  $(\dot{V}/\dot{Q})_{\text{Ext}}$ ,  $(\dot{V}/\dot{Q})_{\dot{V}}$ , and  $(\dot{V}_A/\dot{Q})_{\dot{Q}}$  can be seen to exist when the heterogeneity within the volume element is large. Considering each family of curves individually and neglecting the small effect of  $\lambda_N$ , the relationship between  $(\dot{V}/\dot{Q})_{\text{Ext}}$  and  $(\dot{V}/\dot{Q})_{\dot{Q}}$  at constant  $\dot{V}_1$  (Fig. 4A) is determined by the volume weighting, there being equality between  $(\dot{V}/\dot{Q})_{\text{Ext}}$  and  $(\dot{V}/\dot{Q})_{\dot{Q}}$  when  $V_1 = V_2$  (curve 2) irrespective of the degree of  $\dot{V}/\dot{Q}$  heterogeneity. With a high weighting to compartment 1 ( $V_1 = 10V_2$ , curve 1),  $(\dot{V}/\dot{Q})_{\text{Ext}}$  becomes progressively larger than  $(\dot{V}/\dot{Q})_{\dot{Q}}$  at high values of  $(\dot{V}/\dot{Q})_1/(\dot{V}/\dot{Q})_2$  because of the high weighting given to  $(\dot{V}/\dot{Q})_1$  and vice versa at low values of  $(\dot{V}/\dot{Q})_1/(\dot{V}/\dot{Q})_2$ . The converse occurs when a low weighting is given to compartment 1 ( $10V_1 = V_2$ , curve 3). The effect of maintaining  $\dot{Q}_1$  constant and varying  $\dot{V}_1$  (Fig. 4B to increase the value of  $(\dot{V}/\dot{Q})_{\dot{Q}}$  for a given volume weighting and  $(\dot{V}/\dot{Q})_1/(\dot{V}/\dot{Q})_2$  ratio and thus reduce the value of  $(\dot{V}/\dot{Q})_{\text{Ext}}/(\dot{V}/\dot{Q})_{\dot{Q}}$ . The curves in Fig. 4B therefore bear the same relationship to one

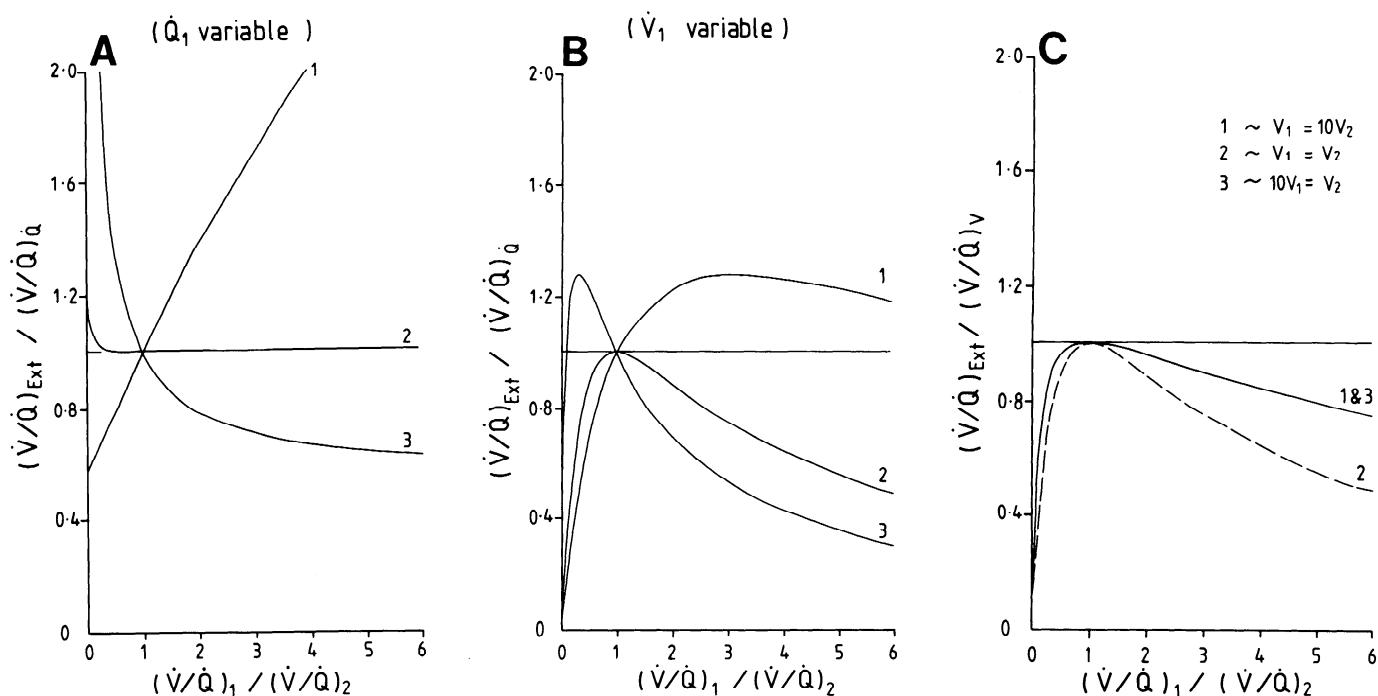


FIG. 4. Relationship between predicted ventilation-to-perfusion ( $\dot{V}/\dot{Q}$ ) ratio obtained using external detection [ $(\dot{V}/\dot{Q})_{\text{Ext}}$ ] and the mean  $\dot{V}/\dot{Q}$  ratio [chosen either to be volume- ( $\dot{V}$ ) or blood flow- ( $\dot{Q}$ ) weighted], for a heterogeneous lung region comprising 2 discrete  $\dot{V}/\dot{Q}$  subpopulations [ $(\dot{V}/\dot{Q})_1$  and  $(\dot{V}/\dot{Q})_2$ ] as the degree of heterogeneity [the ratio  $(\dot{V}/\dot{Q})_1/(\dot{V}/\dot{Q})_2$  changes. Curves are numbered to denote relationship between volumes of the 2 subregions (see inset).

another as those in Fig. 4A but have progressively lower values as  $\dot{V}/\dot{Q}$  heterogeneity increases. Interestingly, the volume-weighted mean  $\dot{V}/\dot{Q}$  ratio is not equal to the measured  $\dot{V}/\dot{Q}$  ratio when  $(\dot{V}/\dot{Q})_1$  and  $(\dot{V}/\dot{Q})_2$  differ (Fig. 4C). This results from the reciprocal relationship between  $(\dot{V}/\dot{Q})_i$  and  $(\dot{V}/\dot{Q})_{\text{Ext.}}$ .

## DISCUSSION

**$\dot{V}D$  and  $\dot{V}/\dot{Q}$  ratio.** The general effect of inspiring alveolar gas of a different composition to that of the resident alveoli (ventilation from the common dead space), as distinct from the inhalation of alveolar gas of the same composition (ventilation from the regional or personal dead space), has been investigated theoretically by Ross and Farhi (12), who showed that  $\dot{V}D_c$  would have the effect of reducing the overall dispersion of alveolar  $O_2$  and  $CO_2$  composition when  $\dot{V}/\dot{Q}$  was heterogeneous throughout the lung. This theme was later extended by Fortune and Wagner (4) to include the exchange of inert gases in a multicompartmental model with special reference to the multiple inert gas elimination technique. They showed that only small changes in the distribution of  $\dot{V}/\dot{Q}$  occurred when  $\dot{V}D_r$  was replaced by  $\dot{V}D_c$  as determined by a 10% decrease in the standard deviation of the recovered  $\dot{V}A/\dot{Q}$  distribution. However, differences of up to 40% were obtained for individual values of  $\dot{V}A/\dot{Q}$  in the range from 0.02 to 0.2. Anthonisen et al. (1), adopting the same basic principle used in this paper (a constant intravenous infusion of  $^{133}\text{Xe}$  and external detection by use of a scintillation detector array) made various corrections for  $\dot{V}D$  by use of a two-compartmental dead-space model, to calculate  $\dot{V}A/\dot{Q}$  and  $\dot{V}GE/\dot{Q}$ , where  $\dot{V}GE (= \dot{V}A + \dot{V}D_c)$  was judged to be the total gas-exchanging ventilation.

Most, if not all, previous work on this subject has been based on the central idea that  $\dot{V}A/\dot{Q}$  is a gold standard against which other measurements should be judged. This is in spite of the fact that  $\dot{V}A$  is a somewhat elusive parameter, in that regionally,  $\dot{V}D$  and  $C_{D_c}$  are unknown, and  $\dot{V}A$  is therefore not an unambiguous indicator of gas transport.

The behavior of  $(\dot{V}A/\dot{Q})_{\text{eff}(^{13}\text{N})_r}$  (Fig. 2) is determined by the composition of the common dead space gas and consequently the  $\dot{V}/\dot{Q}$  ratios of the regions feeding this compartment [ $(\dot{V}A/\dot{Q})_e$  in our illustrative model]. At low  $(\dot{V}A/\dot{Q})_r$  the alveolar concentration of  $^{13}\text{N}$  is high, and the common dead space gas is relatively free of  $^{13}\text{N}$ . The  $\dot{V}A_{\text{eff}}$  is therefore higher than  $\dot{V}A$  and  $(\dot{V}A/\dot{Q})_{\text{eff}(^{13}\text{N})_r}$  is greater than  $(\dot{V}A/\dot{Q})_r$ , the maximum value for the ratio of the two  $\dot{V}/\dot{Q}$  ratios being  $(\dot{V}D_c + \dot{V}A)/\dot{V}A$  or  $\dot{V}T/\dot{V}A$  when  $\dot{V}D_c = \dot{V}D$ . Conversely, as the  $\dot{V}/\dot{Q}$  ratio of the region of interest increases beyond  $(\dot{V}A/\dot{Q})_e$ , the  $^{13}\text{N}$  concentration of the gas inspired from the common dead space [ $(\dot{V}A/\dot{Q})_e = 0.75$ ] is now relatively high, therefore less  $^{13}\text{N}$  is exchanged, the effective  $\dot{V}/\dot{Q}$  ratio falls below  $(\dot{V}A/\dot{Q})_r$ , and the ratio  $(\dot{V}A/\dot{Q})_{\text{eff}(^{13}\text{N})_r} / (\dot{V}A/\dot{Q})_r$  ultimately tends toward zero as  $(\dot{V}A/\dot{Q})_r$  becomes very large. The reason for this fall in  $(\dot{V}A/\dot{Q})_{\text{eff}(^{13}\text{N})_r}$  at high  $(\dot{V}A/\dot{Q})_r$  values (when, for example,  $\dot{Q}_r$  approaches 0) is that  $\dot{V}A$  becomes progressively less involved in  $^{13}\text{N}$  elimination.

Indeed, it is easy to show, by multiplying both sides of Eq. A5 by  $\dot{Q}$ , that  $\dot{V}A_{\text{eff}}$  tends toward zero as  $\dot{Q}_r$  falls to zero (i.e., when  $(\dot{V}A/\dot{Q})_r$  tends toward infinity).

The behavior of  $(\dot{V}A/\dot{Q})_{\text{eff}(^{13}\text{N})_r}$  when  $\dot{Q}_r$  approaches zero is shown in Fig. 3. When  $\dot{Q}_r$  equals zero, both the numerator and denominator of  $(\dot{V}A/\dot{Q})_{\text{eff}(^{13}\text{N})_r}$  are zero, but the ratio is mathematically well defined (as described above) and has a value of 4.32 for the various dead-space parameters used in this example. This means that a value of  $(\dot{V}A/\dot{Q})_{\text{eff}(^{13}\text{N})_r}$  above 4.3 would not be recorded, given these combinations of  $\dot{V}D$  and gas composition, and this value of  $(\dot{V}A/\dot{Q})_{\text{eff}(^{13}\text{N})_r}$  should be considered to be a true estimation of the upper limit of the gas-exchanging  $\dot{V}/\dot{Q}$  ratio for infused  $^{13}\text{N}$  in this example (the approximate expression for a gas of low solubility being  $(\dot{V}A/\dot{Q})_{\text{eff}(\text{max})} = (\dot{V}A/\dot{V}D_c + 1)/(\dot{V}A/\dot{Q})_e$ , from Eq. A5).

The physiological relevance of a finite value for  $(\dot{V}A/\dot{Q})_{\text{eff}}$  at very low blood flows [ $(\dot{V}A/\dot{Q})_r$  very high] can be illustrated by considering the case for  $CO_2$ . Values of  $(\dot{V}A/\dot{Q})_{\text{eff}(CO_2)}$  (Eq. A5) and alveolar partial pressure of  $CO_2$  ( $P_{ACO_2}$ ) [obtained as the effective inspired partial pressure of  $CO_2$  ( $P_{\text{eff}}$ ), Eq. A6, when  $CO_2$  transport via blood is relatively low] vary as the local dead space-to-tidal volume ratio changes. Calculations have been made for the constant conditions  $(\dot{V}A/\dot{Q})_r = 1,000$ ,  $(\dot{V}A/\dot{Q})_e = 0.75$ , and  $\lambda = 9$  (for  $CO_2$ , see below). The result is an approximate hyperbolic relationship between  $(\dot{V}A/\dot{Q})_{\text{eff}(CO_2)}$  and  $P_{ACO_2}$ . A low contribution from  $\dot{V}D$  ( $\dot{V}D_c = \dot{V}D_r = 0.05 \dot{V}T$ ) results in values for  $(\dot{V}A/\dot{Q})_{\text{eff}(CO_2)}$  and  $P_{ACO_2}$  of 150 and 2.3 Torr, whereas a high  $\dot{V}D$  ( $\dot{V}D_c = \dot{V}D_r = 0.45 \dot{V}T$ ) gives values of 2.9 and 36 Torr, respectively. Although  $\dot{V}D$  is, in reality, an unknown quantity (especially on a regional basis), it is automatically accounted for by  $(\dot{V}A/\dot{Q})_{\text{eff}}$ . This parameter thus provides an insight into the gas-exchanging state of the alveolus, since it predicts the local  $P_{ACO_2}$ , and it is the prevailing  $P_{ACO_2}$  that, in part, determines how much  $CO_2$  is removed from the blood in such a region. The knowledge that  $(\dot{V}A/\dot{Q})_r = 1,000$  in itself would not aid in the prediction of  $P_{ACO_2}$ .

**Relationship between  $(\dot{V}A/\dot{Q})_{\text{eff}(^{13}\text{N})_r}$  and  $(\dot{V}A/\dot{Q})_r$ ,  $(\dot{V}A/\dot{Q})_{\text{eff}(O_2)_r}$  and  $(\dot{V}A/\dot{Q})_{\text{eff}(CO_2)_r}$ .** Although it is important to compare  $(\dot{V}A/\dot{Q})_{\text{eff}(^{13}\text{N})_r}$  with  $(\dot{V}A/\dot{Q})_r$ , a major interest may actually be in the transport of  $O_2$  and  $CO_2$ . The true gas-exchanging  $\dot{V}/\dot{Q}$  ratios for these gases have been calculated by use of the concept of effective ventilation and an estimation of alveolar partial pressure of  $O_2$  ( $P_{AO_2}$ ) and  $P_{ACO_2}$  by use of a computerized version of the common quadrant diagram (11, 14). The corresponding curves for the two gases are shown in Fig. 2. Broadly speaking, both behave in a similar manner to ideal gases, in that the shapes of the two curves are similar to that for  $^{13}\text{N}$ . However, there is a slight systematic variation in both their effective solubility coefficients, as a function of  $(\dot{V}A/\dot{Q})_r$ , which range from 0.3 to 0.8 for  $O_2$  and from 5 to 7 for  $CO_2$  (calculated from Fig. 2). Departure of the behavior of the two gases from that of an ideal gas is ascribed to the shapes of their dissociation curves. Of significance is the fact that  $O_2$  has gas-exchanging characteristics that are very close to infused  $^{13}\text{N}$  and

$(\dot{V}_A/\dot{Q})_{\text{eff}(O_2)_r}$ , can, to a good approximation, be equated to  $(\dot{V}_A/\dot{Q})_{\text{eff}(^{13}\text{N})_r}$ . The behavior of  $\text{CO}_2$ , on the other hand, is rather less like  $^{13}\text{N}$  and is more inclined toward  $(\dot{V}_A/\dot{Q})_r$ . This disparity is more pronounced at low  $\dot{Q}_r$  [high  $(\dot{V}_A/\dot{Q})_r$ ] values, which indicates that  $\dot{V}/\dot{Q}$  measured with  $^{13}\text{N}$  is not an ideal indicator of  $(\dot{V}_A/\dot{Q})_{\text{eff}(\text{CO}_2)}$  under such conditions (see previous section). The overall conclusion is that measurements of  $\dot{V}/\dot{Q}$ , dependent on relatively insoluble inert gas techniques, may underestimate the range of  $(\dot{V}_A/\dot{Q})_r$ , but will not underestimate the range of  $(\dot{V}_A/\dot{Q})_{\text{eff}}$  for  $\text{O}_2$  and  $\text{CO}_2$  to anything like the same extent. Thus  $\dot{V}\dot{D}$ , which regionally is virtually an unknown quantity, has far less a confounding influence on these measurements of  $\dot{V}/\dot{Q}$  when the interest is in net gas transport rather than bulk flow.

**Heterogeneity of  $\dot{V}/\dot{Q}$  within the volume element.** The determination of regional  $\dot{V}/\dot{Q}$  described in this paper requires the regional measurement of  $^{13}\text{N}$  concentration (with respect to the alveolar gas volume). This is achieved with positron emission tomography (PET) as described in detail in the accompanying paper. The spatial resolution of modern multiplane PET scanners is now of the order of 4–6 mm full width at half-maximum response to a line source of radioactivity (FWHM), which means that isotope concentrations can be accurately measured in lung volumes down to 2 cm<sup>3</sup>. Nevertheless, significant mismatching between  $\dot{V}$  and  $\dot{Q}$  may occur at a microscopic level, and any volume element viewed, however small, may include a wide dispersion of  $\dot{V}/\dot{Q}$  ratios. Any steady-state technique employing external detection is forced to average this dispersion in some way, thereby providing weighted  $\dot{V}/\dot{Q}$  values. In Fig. 4, the behavior of the ratio  $(\dot{V}/\dot{Q})_{\text{Ext}}$  to  $(\dot{V}/\dot{Q})_{\text{mean}}$  varies not only as a function of the ratio  $(\dot{V}/\dot{Q})_1$  to  $(\dot{V}/\dot{Q})_2$  but also on how  $(\dot{V}/\dot{Q})_{\text{mean}}$  is defined. In terms of the relationship of  $\dot{V}/\dot{Q}$  to blood gases, the perfusion-weighted  $\dot{V}/\dot{Q}$  is appropriate [ $(\dot{V}/\dot{Q})_{\dot{Q}}$ , see Eq. A9], but in terms of assessing the extent of pathology in the lung, a volume-weighted mean [ $(\dot{V}/\dot{Q})_V$ ] is more relevant and is the approach taken when analyzing interregional differences with this PET technique.

The mean “pixel”  $\dot{V}/\dot{Q}$  ratio obtained with PET is derived from the volume-weighted  $\dot{Q}/\dot{V}$  ratio and in this respect deviates from the volume-weighted  $\dot{V}/\dot{Q}$  ratio, as shown in Fig. 4C. However, these differences are clearly related to the way in which the data are presented, since virtually no difference would exist if the gas-exchanging ability of a given lung region was to be assessed in terms of the  $\dot{Q}/\dot{V}$  ratio instead of  $\dot{V}/\dot{Q}$  ratio, except at very low values of  $\dot{V}/\dot{Q}$  (see Eq. A13).

Considering differences between  $(\dot{V}/\dot{Q})_{\text{Ext}}$  and  $(\dot{V}/\dot{Q})_{\dot{Q}}$ , the most realistic pathophysiological reason for  $\dot{V}/\dot{Q}$  to change significantly, within a small volume of lung, is because of a fall in either  $\dot{V}$  or  $\dot{Q}$ , resulting in a decrease or increase in  $\dot{V}/\dot{Q}$ , respectively. This limits the relevant regions in Fig. 4, A and B, to  $(\dot{V}/\dot{Q})_1/(\dot{V}/\dot{Q})_2$  ratios greater than unity in Fig. 4A and less than unity in Fig. 4B. Clearly, from these curves, the effect of  $\dot{V}/\dot{Q}$  heterogeneity within the volume element is to introduce a progressive divergence between  $(\dot{V}/\dot{Q})_{\text{Ext}}$  and  $(\dot{V}/\dot{Q})_{\dot{Q}}$ , depending on the volume weighting of the  $\dot{V}/\dot{Q}$  distribution.

## APPENDIX 1

### Derivation of Relationships Between $(\dot{V}_A/\dot{Q})_{\text{eff}}$ and $(\dot{V}_A/\dot{Q})_r$

For the purpose of this analysis the following simplifying assumptions are made. 1) Total dead-space ventilation ( $\dot{V}\dot{D} = \Sigma\dot{V}\dot{D}_i$ ) consists of two components only: a) regional dead-space gas ( $\dot{D}_r$ ) with a tracer concentration ( $\text{CD}_r$ ) equal to that of the alveolar gas in the volume element of the region of interest ( $\text{CA}_r$ ) and b) common dead-space gas ( $\dot{D}_c$ ) with a tracer concentration ( $\text{CD}_c$ ) determined by the  $\dot{V}/\dot{Q}$  ratio of lung external to the volume element. 2) The common dead-space is homogeneous with respect to its gas composition, representing gas expired from a lung region external to the region of interest with a single  $\dot{V}/\dot{Q}$  ratio,  $(\dot{V}/\dot{Q})_e$ . 3) In the volume element, there is a proportional relationship between the  $\dot{V}\dot{D}_c$  and  $\dot{V}_A$  such that  $F_c = \dot{V}\dot{D}_c/\dot{V}_A$ . 4) RQ is unity for each region, and thus  $\dot{V}_A(\text{inspired}) = \dot{V}_A(\text{expired})$ . [The effect of this simplifying assumption is most apparent at low values of  $\dot{V}/\dot{Q}$  and when  $\dot{V}_A(\text{eff})$  is compared with inspired  $\dot{V}_A$ . For  $^{13}\text{N}$  and  $\text{CO}_2$  (when  $\dot{V}_A(\text{eff})$  is involved in the elimination of gas and therefore expiratory in nature), there is an overestimation of the true  $\dot{V}_A(\text{eff})$  by ~10% when  $\dot{V}/\dot{Q} = 0.1$ . Conversely for  $\text{O}_2$  (where  $\dot{V}_A(\text{eff})$  is inspiratory), the effect is to underestimate  $\dot{V}_A(\text{eff})$  by ~6% at this value of  $\dot{V}/\dot{Q}$ ].

Substituting Eq. 2 into Eq. 3 to eliminate  $\dot{V}\dot{D}_{\text{eff}}$  and form a general equation for a region  $r$  gives

$$\dot{V}_A(\text{eff})_r = (\dot{V}_A)_r + \dot{V}\dot{D}_r + \dot{V}\dot{D}_c - (\dot{V}\dot{D}_r\text{CD}_r + \dot{V}\dot{D}_c\text{CD}_c)/\text{CA}_r \quad (\text{A1})$$

Because  $\text{CD}_r = \text{CA}_r$  (assumption 1, above) then

$$\dot{V}_A(\text{eff})_r = \dot{V}_A)_r + \dot{V}\dot{D}_c (1 - \text{CD}_c/\text{CA}_r) \quad (\text{A2})$$

$(\dot{V}_A/\dot{Q})_{\text{eff}}$  can then be expressed in terms of  $(\dot{V}_A/\dot{Q})_r$  by eliminating  $\dot{V}\dot{D}_c$  from Eq. A2 (see assumption 3) and dividing throughout by  $\dot{Q}$ , thus

$$(\dot{V}_A/\dot{Q})_{\text{eff}} = (\dot{V}_A/\dot{Q})_r [1 + F_c(1 - \text{CD}_c/\text{CA}_r)] \quad (\text{A3})$$

### Equation for an Inert Gas

Equation A3 is of general applicability to different gases and can be used analytically for any inert gas ( $x$ ) with a first-order solubility coefficient ( $\lambda_x$ ) by substituting for  $\text{CD}_c$  and  $\text{CA}_r$  by use of the relationship expressed by Eq. 4. Thus

$$\text{CD}_{c(x)}/\text{CA}_{r(x)} = [(\dot{V}_A/\dot{Q})_{\text{eff}(x)} + \lambda_x]/[(\dot{V}_A/\dot{Q})_e + \lambda_x] \quad (\text{A4})$$

[It is important to note here that although the common dead-space tracer concentration [ $\text{CD}_{c(x)}$ ] is related to the  $\dot{V}_A/\dot{Q}$  ratio of the external lung region,  $(\dot{V}_A/\dot{Q})_e$ , since  $(\dot{V}_A/\dot{Q})_{\text{eff}(x)_e} = (\dot{V}_A/\dot{Q})_e$ , the concentration of tracer in the alveolar gas of the region of interest [ $\text{CA}_{r(x)}$ ] is related to the effective  $\dot{V}/\dot{Q}$  ratio of the region of interest  $(\dot{V}_A/\dot{Q})_{\text{eff}(x)_r}$ . Substituting Eq. A4 into Eq. A3 and solving for  $(\dot{V}_A/\dot{Q})_{\text{eff}(x)_r}$  gives the operational equation

$$(\dot{V}_A/\dot{Q})_{\text{eff}(x)_r} = (\dot{V}_A/\dot{Q})_r [(1 + F_c)(\dot{V}_A/\dot{Q})_e + \lambda_x]/[(\dot{V}_A/\dot{Q})_e + F_c(\dot{V}_A/\dot{Q})_r + \lambda_x] \quad (\text{A5})$$

### Equation for $\text{CO}_2$

Equation A3 cannot be solved algebraically for  $\text{CO}_2$ , since the dissociation curve for this gas is not linear. The  $\text{PCO}_2$  in the common dead-space gas [ $\text{PD}_{c(\text{CO}_2)}$ ] and in the alveolar gas of the region of interest [ $\text{PA}_{r(\text{CO}_2)}$ ] can be obtained (as described above in the main body of the paper) using the multiple-compartment  $\dot{V}/\dot{Q}$  model of West and Wagner (14) and substituted directly into Eq. A3. To use this computer program, a calculation of the  $P_{\text{eff}}$  of  $\text{O}_2$  and  $\text{CO}_2$  was necessary and was

made using simple dilution theory and the various dead-space ventilations (12) from the equation

$$P_{\text{eff}} = (\dot{V}_A/\dot{V}_T)P_{\text{atm}} + (\dot{V}_{D_r}/\dot{V}_T)PD_r + (\dot{V}_{D_c}/\dot{V}_T)PD_c \quad (A6)$$

Equation for  $O_2$

The calculation of  $(\dot{V}_A/\dot{Q})_{\text{eff}(O_2)}$ , requires a slightly different approach, since  $O_2$  is transported by ventilation bidirectionally, both into and out of the lung. The effective ventilation for  $O_2$  [ $\dot{V}_{A_{\text{eff}}(O_2)}$ ] is therefore defined in terms of the atmospheric partial pressure [ $P_{\text{atm}}(O_2)$ ] and the alveolar partial pressure for the region of interest ( $P_{A_r}(O_2)$ ). Thus the ventilation equation can be written

$$\begin{aligned} \dot{V}_{A_{\text{eff}}(O_2)}(P_{\text{atm}}(O_2) - P_{A_r}(O_2)) \\ = \dot{V}_{A_r}P_{\text{atm}}(O_2) + \dot{V}_{D_r}P_{A_r}(O_2) + \dot{V}_{D_c}PD_c(O_2) - \dot{V}_T P_{A_r}(O_2) \end{aligned} \quad (A7)$$

[In this equation, the  $PO_2$  has been used to denote the fractional  $O_2$  content of alveolar gas, since barometric pressure (PB), which occurs in the true expression ( $P_{x(O_2)}/PB$ ), appears in each term in the equation and therefore cancels out.]

Equation A7 can be reduced, simplified, and converted into  $\dot{V}/\dot{Q}$  to give the following operational equation for  $(\dot{V}_A/\dot{Q})_{\text{eff}(O_2)}$ ,

$$\begin{aligned} (\dot{V}_A/\dot{Q})_{\text{eff}(O_2)} = (\dot{V}_A/\dot{Q})_r \{1 + F_c [P_e(O_2) \\ - P_{A_r}(O_2)] / [P_{\text{atm}}(O_2) - P_{A_r}(O_2)]\} \end{aligned} \quad (A8)$$

where  $P_e(O_2)$ , the  $PO_2$  in the external lung compartment, is equal to the common dead-space  $PO_2$  [ $PD_c(O_2)$ ].

## APPENDIX 2

### Derivation of Equations for Heterogeneity of $\dot{V}/\dot{Q}$

The mean values of  $\dot{V}/\dot{Q}$ , weighed for  $\dot{Q}$  or volume (V) are defined as follows

$$\begin{aligned} (\dot{V}/\dot{Q})_{\dot{Q}} &= \Sigma \dot{Q}_i (\dot{V}/\dot{Q})_i / \Sigma \dot{Q}_i \\ &= \Sigma \dot{V}_i / \Sigma \dot{Q}_i \end{aligned} \quad (A9)$$

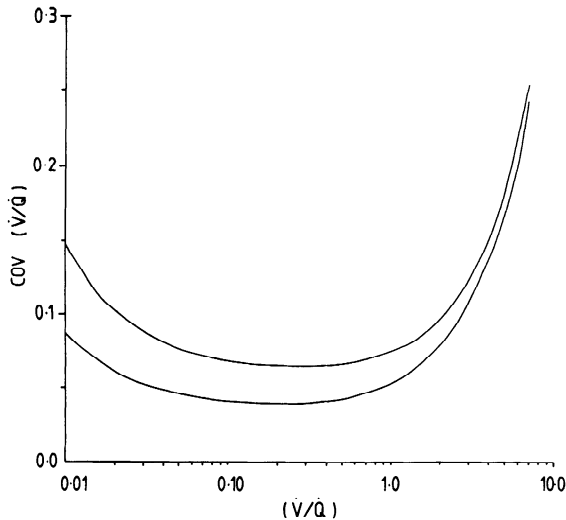


FIG. 5. Relative error [coefficient of variation (COV)] in measurement of ventilation-to-perfusion ratio ( $\dot{V}/\dot{Q}$ ) as a function of  $\dot{V}/\dot{Q}$ . Bottom curve, errors excluding uncertainty in measurement of mixed venous  $^{13}N$  concentration (relevant to interregional comparisons of  $\dot{V}/\dot{Q}$ ). Top curve, total error of measurement.

and

$$\begin{aligned} (\dot{V}/\dot{Q})_V &= \Sigma V_i (\dot{V}/\dot{Q})_i / \Sigma V_i \\ &= \Sigma F_{V_i} (\dot{V}/\dot{Q})_i \end{aligned} \quad (A10)$$

where  $F_{V_i} = (V_i/\Sigma V_i)$  corresponds to the fractional volume of the lung region associated with a ventilation-to-perfusion ratio ( $\dot{V}/\dot{Q}$ )<sub>*i*</sub>.

The expression for the  $\dot{V}/\dot{Q}$  ratio measured using external detection [i.e.,  $(\dot{V}/\dot{Q})_{\text{Ext}}$ ] is derived from Eq. 5

$$(\dot{V}/\dot{Q})_{\text{Ext}} = C\bar{V}/C\bar{A} - \lambda_N \quad (A11)$$

where  $C\bar{A}$ , the measured  $^{13}N$  concentration of the region, is related to the concentration in the individual subregions ( $C_{A_i}$ ) and their respective alveolar gas volumes ( $V_{A_i}$ ) by the equation

$$\begin{aligned} C\bar{A} &= \Sigma V_{A_i} C_{A_i} / \Sigma V_{A_i} \\ &= \Sigma F_{V_i} C_{A_i} \end{aligned} \quad (A12)$$

when the microscopic distribution of lung tissue and blood is uniform throughout the volume element. Combining Eqs. A11 and A12 to eliminate  $C\bar{A}$  and substituting for  $C_{A_i}$  by use of Eq. 5 gives

$$(\dot{V}/\dot{Q})_{\text{Ext}} = 1/\Sigma \{F_{V_i} / [(\dot{V}/\dot{Q})_i + \lambda_N]\} - \lambda_N \quad (A13)$$

## APPENDIX 3

### Error Propagation in the $\dot{V}/\dot{Q}$ Equation

Equation 4 can be rewritten in terms of the measured scan data to give

$$(\dot{V}_A/\dot{Q})_{\text{eff}(^{13}N)} = C\bar{V}V_A / [S_{^{13}N(\text{total})} - S_{^{13}N(\text{vacc})}] - \lambda_N \quad (A14)$$

where  $S_{^{13}N(\text{total})}$  is the regional distribution of  $^{13}N$  ( $\mu\text{Ci}$  per unit volume of thorax) and  $V_A$  is the regional pulmonary gas volume (ml per unit volume of thorax).  $S_{^{13}N(\text{vacc})}$  is the background  $^{13}N$  activity included in  $S_{^{13}N(\text{total})}$  and originates from blood containing  $^{13}N$  (at a concentration  $C\bar{V}$ ) upstream of the alveolus. This vascular moiety can be calculated as  $F_a C\bar{V} V_B$ , where  $F_a$  is the fraction of the regional blood volume ( $V_B$ ) upstream of the alveolus.  $F_a$  has been assigned a value of 0.4 (see companion paper). Differentiation of this equation allows the coefficient of variation (COV) of the measured values of  $\dot{V}/\dot{Q}$  to be expressed in terms of the COV's of the component parameters, thus

$$\begin{aligned} \text{COV}_{(\dot{V}/\dot{Q})} &= \left[ \text{COV}_{V_A}^2 + (1 - A)^2 \left( \text{COV}_{C\bar{V}}^2 \right. \right. \\ &\quad \left. \left. + \text{COV}_{^{13}N}^2 \right) + A^2 \text{COV}_{V_B}^2 \right]^{1/2} \frac{Ak}{(\dot{V}/\dot{Q})} \end{aligned} \quad (A15)$$

where  $A = (\dot{V}/\dot{Q} + \lambda_N)/k$  and  $k = V_A/F_a V_B$ .

The fractional errors in the measurements of  $V_A$ ,  $V_B$ , and  $C\bar{V}$  are independent of  $\dot{V}/\dot{Q}$  and for a typical lung region of interest ( $2 \times 2 \text{ cm}^2$ ) are estimated to be 0.035, 0.010, and 0.047, respectively, when the number of accumulated counts in the transmission, blood volume, and  $^{13}N$  steady-state emission scans are  $10 \times 10^6$ ,  $2 \times 10^6$ , and  $0.5 \times 10^6$ , respectively. The value of  $\text{COV}_{^{13}N}$  is, however, related to regional  $\dot{V}/\dot{Q}$ , since a high value of  $\dot{V}/\dot{Q}$  is associated with a low concentration of  $^{13}N$  and a correspondingly high statistical uncertainty. For a uniform distribution of activity throughout the lungs, the COV for the measurement of isotope concentration in a  $2 \times 2\text{-cm}^2$  region is  $\sim 0.03$  for the accumulation of  $0.5 \times 10^6$  coincidence events. Therefore, the following first-order approximation between

$\text{COV}_{^{13}\text{N}}$  and  $\dot{V}/\dot{Q}$  can be made (2)

$$\text{COV}_{^{13}\text{N}} = 0.03[(\dot{V}/\dot{Q} + \lambda_{\text{N}})/(0.8 + \lambda_{\text{N}})]^{3/2} \quad (\text{A16})$$

where the value 0.8 is the mean  $\dot{V}/\dot{Q}$  ratio for normal subjects.

$\text{COV}_{(\dot{V}/\dot{Q})}$  was calculated using Eqs. A15 and A16 and is shown plotted in Fig. 5 as a function of  $\dot{V}/\dot{Q}$ . At low values of  $\dot{V}/\dot{Q}$  the relative error is high because of the subtraction of  $\lambda_{\text{N}}$  from the ratio  $\text{C}\bar{\text{V}}/\text{CA}$ , which is itself tending toward a value of  $\lambda_{\text{N}}$ . In the  $\dot{V}/\dot{Q}$  range from 0.1 to 1.0,  $\text{COV}_{(\dot{V}/\dot{Q})}$  is relatively constant, but as  $\dot{V}/\dot{Q}$  increases further, the errors in the measurement also increase because of the statistical uncertainty in the measurement of  $^{13}\text{N}$  concentration.

Present address of S. O. Valind and P. E. Wollmer: Dept. of Clinical Physiology, University of Lund, S-221 85 Lund, Sweden. Present address of L. H. Brudin: Dept. of Clinical Physiology, Kalmar Hospital, S-391 85, Kalmar, Sweden.

Address for reprint requests: C. G. Rhodes, MRC Cyclotron Unit, Hammersmith Hospital, London W12 OHS, UK.

Received 16 November 1987; accepted in final form 2 November 1988.

## REFERENCES

1. ANTHONISEN, N. R., M. B. DOLOVICH, AND D. V. BATES. Steady state measurement of regional ventilation to perfusion ratios in normal man. *J. Clin. Invest.* 45: 1349-1356, 1966.
2. BUDINGER, T. F., S. E. DERENZO, W. L. GREENBERG, G. T. GULLBERG, AND R. H. HUESMAN. Quantitative potentials of dynamic emission computed tomography. *J. Nucl. Med.* 19: 309-315, 1978.
3. FARHI, L. E. Elimination of inert gas by the lung. *Respir. Physiol.* 3: 1-11, 1967.
4. FORTUNE, J. B., AND P. D. WAGNER. Effects of common dead space on inert gas exchange in mathematical models of the lung. *J. Appl. Physiol.* 47: 896-906, 1979.
5. HARF, A., T. PRATT, AND J. M. B. HUGHES. Regional distribution of  $\dot{V}_A/\dot{Q}$  in man at rest and with exercise measured with krypton-81m. *J. Appl. Physiol.* 44: 115-123, 1978.
6. HILL, D. W. Properties of liquid gases and vapours. In: *Physics Applied to Anaesthesia* (4th ed.). London: Butterworth, 1980, chapt. 5, p. 209.
7. KETY, S. S. The theory and applications of the exchange of inert gas at the lungs and tissues. *Pharmacol. Rev.* 3: 1-41, 1951.
8. LAVENDER, J. P., A. M. AL-NAHHAS, AND M. J. MYERS. Ventilation perfusion ratios of the normal supine lung using emission tomography. *Br. J. Radiol.* 57: 141-146, 1984.
9. PHELPS, M. E., E. J. HOFFMAN, S. C. HUANG, AND D. E. KUHL. ECAT: a new computerized tomographic imaging system for positron-emitting radiopharmaceuticals. *J. Nucl. Med.* 19: 635-647, 1978.
10. RHODES, C. G., S. O. VALIND, L. H. BRUDIN, P. E. WOLLMER, T. JONES, P. D. BUCKINGHAM, AND J. M. B. HUGHES. Quantification of regional  $\dot{V}/\dot{Q}$  ratios in humans by use of PET. II. procedure and normal values. *J. Appl. Physiol.* 66: 1905-1913, 1989.
11. RILEY, R. L., AND S. PERMUT. The four quadrant diagram for analyzing the distribution of gas and blood in the lung. In: *Handbook of Physiology. Respiration*. Washington, DC: Am. Physiol. Soc., 1965, sect. 3, vol. II, chapt. 56, p. 1413-1423.
12. ROSS, B. B., AND L. E. FARHI. Dead-space ventilation as a determinant in the ventilation-perfusion concept. *J. Appl. Physiol.* 15: 363-371, 1960.
13. WAGNER, P. D., H. A. SALTZMAN, AND J. B. WEST. Measurement of continuous distributions of ventilation-perfusion ratios: theory. *J. Appl. Physiol.* 36: 588-599, 1974.
14. WEST, J. B., AND P. D. WAGNER. Pulmonary gas exchange. In: *Bioengineering Aspects of the Lung*. New York: Dekker, 1977, vol. 3, p. 361-457. (Lung Biol. Health Dis. Ser.)